STARS

University of Central Florida
STARS

Faculty Bibliography 2010s

Faculty Bibliography

1-1-2010

Photoassociation of a cold-atom-molecule pair: Long-range quadrupole-quadrupole interactions

M. Lepers

O. Dulieu

Viatcheslav Kokoouline
University of Central Florida

Recommended Citation

Showcase of Text, Archives, Research & Scholarship

Photoassociation of a cold-atom–molecule pair: Long-range quadrupole-quadrupole interactions

M. Lepers,[1,*] O. Dulieu,[1] and V. Kokoouline[1,2]

[1]*Laboratoire Aimé Cotton, CNRS, UPR3321, Bâtiment 505, Université Paris-Sud,*
F-91405 Orsay Cedex, France
[2]*Department of Physics, University of Central Florida, Orlando, Florida 32816, USA*

The general formalism of the multipolar expansion of electrostatic interactions is applied to the calculation of the potential energy between an excited atom (without fine structure) and a ground-state diatomic molecule at large mutual separations. Both partners exhibit a permanent quadrupole moment so that their mutual long-range interaction is dominated by a quadrupole-quadrupole term, which is attractive enough to bind trimers. Numerical results are given for an excited $Cs(6\,^2P)$ atom and a ground-state Cs_2 molecule. The prospects for achieving photoassociation of a cold-atom–dimer pair are thus discussed and found promising. The formalism can be generalized to the long-range interaction between molecules to investigate the formation of cold tetramers.

I. INTRODUCTION

Since it was proposed by Thorsheim *et al.* [1] in 1987, and first observed for sodium [2] and for rubidium [3] atoms in 1993, the photoassociation (PA) of pairs of ultracold atoms has had a tremendous impact on research in atomic, molecular, and optical physics at low temperatures. There are several recent review articles devoted to the various aspects of PA [4–7]; therefore, we briefly recall in what follows some of the main features of the PA process, which gave rise to a new high-resolution spectroscopic technique, that is, the PA spectroscopy. Due to their extremely low relative kinetic energy, atoms from an ultracold gas can be associated via a quasiresonant free-bound dipolar transition to form an electronically excited molecule, which is often created in a highly excited rovibrational level. As the PA process is mainly controlled by the long-range electrostatic interactions between cold atoms, it has been used as a high-resolution spectroscopy technique for highly excited rovibrational levels. Such levels observed using PA correspond to vibrational motion of a molecule with much larger extension than the usual chemical bond [8–12]. Such molecules with a very large amplitude of vibration were predicted 15 years before the mentioned experiments [13,14]. The spectroscopy of the highly excited rovibrational levels of photoassociated dimers made it possible, in particular, to determine the most accurate values of the radiative lifetime of the first excited state of alkali-metal atoms (see, for instance, [15]). Another example of PA application is the formation of stable ultracold molecules, reported initially for Cs_2 [16] and later for many other homonuclear and heteronuclear alkali-metal diatomic molecules [17–24].

With the improvement of the experimental techniques at ultracold temperatures, the study of the quantum dynamics of few-body systems in the ultracold regime has become possible, as illustrated by the recent observations of cold collisions between atoms and molecules [25–29]. Such phenomena attract at present a lot of interest as they represent the first manifestation of a novel ultracold chemistry, which is controlled by the quantum nature of the colliding partners

[30,31]. In particular, at certain conditions, the ultracold few-body dynamics exhibits universal (i.e., species-independent) properties for long-range bound states and resonances (see, for example, Refs. [32,33] and references therein), nowadays referred to as the Efimov physics [34,35]. The Efimov states have recently been observed experimentally [36–38].

All these developments concern atoms and molecules in their electronic ground state. The purpose of the present study, as the first of a series of articles, is to investigate the next step toward ultracold chemistry: the association of ultracold atoms and molecules with a laser field to create weakly bound trimers or tetramers in an excited electronic state. Just as for pairs of atoms, the PA probability is determined by the long-range interactions between the colliding partners. Here, we consider the long-range interaction between a $^1\Sigma_g^+$ molecule in a given rovibrational level (v_d, j) with an atom in a P electronic level without fine structure. This situation will be illustrated with the interaction between a ground-state Cs_2 molecule and an excited $Cs(6\,^2P)$ atom, but can be easily generalized to other species. The leading term of this interaction at large interparticle distances R is a quadrupole-quadrupole term varying as R^{-5}. The present work can also be viewed as a step beyond several related studies. The quadrupole-quadrupole interaction between two excited ^2P atoms has been calculated for alkali-metal atom pairs [39] and for the LiB molecule [40]. In Refs. [41,42], the van der Waals interaction (varying as R^{-6}) between alkali-metal dimers in the $(v_d = 0, j = 0)$ level of their lowest triplet state and a ground-state alkali-metal atom has been determined, while in Refs. [43,44] the interaction between a $^2\Pi$ molecule and a ^3P atom *at fixed geometries* is obtained as a sum of a dipole-quadrupole term (in R^{-4}) and a quadrupole-quadrupole term (in R^{-5}).

In Sec. II, we briefly review the main ingredients of the perturbative approach based on the multipolar expansion of the long-range interaction between the two fragments. Section III is devoted to the calculation of C_5 coefficients of the long-range behavior of molecular potentials. We consider the general case of an arbitrary rotational state j of the dimer as well as give an analytical solution for the particular case of $j = 1$. Atomic units (a.u.) for distances (1 a.u. = 0.052 917 7 nm) and for energies (1 a.u. = 219 474.631 37 cm^{-1}) are used throughout the article, unless otherwise stated.

_____
*maxence.lepers@u-psud.fr

II. INTERACTION POTENTIAL AND PERTURBATION THEORY

We start the description of the present theory from the general case, as for instance in Refs. [43,45,46]. We consider two charge distributions, A and B, far from each other such that they do not overlap with each other. A criterion for such a condition is given by the so-called Le Roy radius [47,48] defined as $R_{LR} = 2(\sqrt{\langle r_A^2 \rangle} + \sqrt{\langle r_B^2 \rangle})$, where $\langle r_A^2 \rangle$ and $\langle r_B^2 \rangle$ are the averaged squared distances of the outermost electron from the origin of each charge distribution A and B, respectively. The electrostatic potential energy of interaction between A and B can be written as an expansion over products of multipole moments of A and B located at a distance R from each other:

$$\hat{V}_{AB}(R) = \sum_{L_A, L_B=0}^{+\infty} \sum_{M=-L_<}^{L_<} \frac{1}{R^{1+L_A+L_B}}$$
$$\times f_{L_A L_B M} \hat{Q}_{L_A}^M(\hat{r}_A) \hat{Q}_{L_B}^{-M}(\hat{r}_B), \quad (1)$$

where $L_< = \min(L_A, L_B)$. The operator $\hat{Q}_{L_X}^M(\hat{r}_X)$ is associated with the 2^{L_X}-pole of the charge distribution X ($X = A$ or B), expressed in the body-fixed coordinate system (CS) with the origin at the center of mass of X,

$$\hat{Q}_{L_X}^M(\hat{r}_X) = \sqrt{\frac{4\pi}{2L_X+1}} \sum_{i \in X} q_i \hat{r}_i^{L_X} Y_{L_X}^M(\hat{\theta}_i, \hat{\phi}_i), \quad (2)$$

where q_i is the value of each charge i composing the distribution X. The two coordinate systems (centered at A and B) are assumed to have parallel axes with the Z axis that goes from the center of mass of A toward B (see Fig. 1). This choice of Z implies in Eqs. (1) and (2) that $M_A = -M_B \equiv M$,
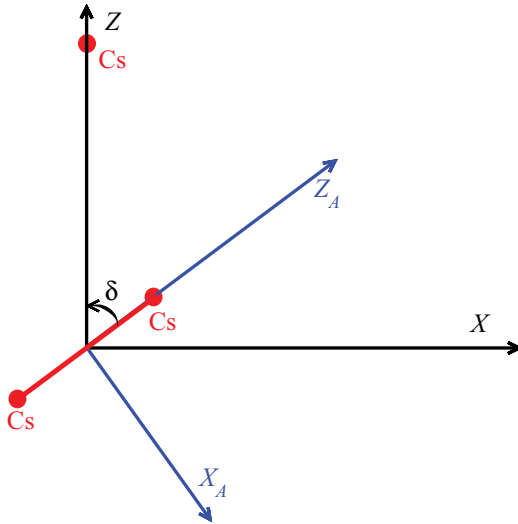

FIG. 1. (Color online) The two coordinate systems, $X_A Y_A Z_A$ (D-CS) and XYZ (T-CS), defined for the dimer and for the trimer, respectively. The Y and Y_A axes coincide and point into the plane of the figure. The subsystem A in this figure is the Cs$_2$ molecule; the subsystem B is the Cs atom. The T-CS is related to the laboratory coordinate system ($\tilde{x}\tilde{y}\tilde{z}$) by the usual Euler angles (α, β, γ), not represented here.

where M_A and M_B are the projections of L_A and L_B, so that the factor $f_{L_A L_B M}$ is equal to

$$f_{L_A L_B M} = \frac{(-1)^{L_B}(L_A + L_B)!}{\sqrt{(L_A+M)!(L_A-M)!}} \frac{1}{\sqrt{(L_B+M)!(L_B-M)!}}. \quad (3)$$

The energy of interaction between the two charge distributions is calculated using perturbation theory. To the lowest (zeroth) order of perturbation theory, the two systems are independent and the total energy is the sum of the individual energies,

$$E_0^0 = E_{A0}^0 + E_{B0}^0, \quad (4)$$

and the total wave function is the product of individual wave functions,

$$\left| \Psi_0^0 \right\rangle = \left| \Psi_{A0}^0 \right\rangle \left| \Psi_{B0}^0 \right\rangle. \quad (5)$$

In Eqs. (4) and (5) and in what follows, the superscript labels the perturbation order and the subscript labels the unperturbed states.

In the present study, the system A is the alkali-metal dimer and B is the alkali-metal atom. We consider the dimer in a vibrational level v_d of its ground electronic state $|X\,^1\Sigma_g^+\rangle$, and in an arbitrary rotational state $|j, m_j\rangle$. In order to investigate a realistic approach for atom-molecule PA, we consider the atom B with a single outer electron being excited to the p state $|n, \ell = 1, \lambda\rangle$. However, we ignore in the following the fine structure of the excited atom for clarity, as discussed later in the text. The projections m_j and λ are defined with respect to the Z axis. The energy origin corresponds to an infinite separation between the atom and the dimer. Thus, the unperturbed energy reduces to

$$E_0^0 = B_{v_d} j(j+1), \quad (6)$$

where B_{v_d} is the rotational constant of the dimer in its vibrational level v_d. The atomic state of B is expressed in the LS coupling case, because the operators in the interaction potential of Eq. (1) act only on the coordinate part of wave functions. The first-order correction E_0^1 to the energy is due to the permanent multipoles of A and B. In our case, both distributions exhibit a permanent quadrupole moment in their body-fixed frame so that the most important contribution comes from the quadrupole-quadrupole interaction with an asymptotic coefficient C_5,

$$E_0^1 = \frac{C_5}{R^5}. \quad (7)$$

III. CALCULATION OF THE C_5 COEFFICIENT

The C_5 coefficient is calculated for arbitrary values of m_j and λ, using the degenerate perturbation theory. We define two body-fixed CSs (Fig. 1). The first CS (which we call the dimer CS, or D-CS) with axes X_A, Y_A, and Z_A has as the origin the center of mass of the dimer. The Z_A axis is the dimer axis and the Y_A axis is orthogonal to the plane of the trimer. The second CS (trimer CS, or T-CS) with axes XYZ is such that the X, Z axes are also (as X_A and Z_A)

in the plane of the trimer, while Z is oriented from the center of the dimer toward the atom B; the Y_A and Y axes are identical. The T-CS is deduced from the D-CS by a rotation with an angle δ around the Y axis.

The perturbation Hamiltonian $V_{AB}^{qq}(R)$ for the quadrupole-quadrupole interaction is given by setting $L_A = L_B = 2$ in Eq. (1):

$$\hat{V}_{AB}^{qq}(R) = \frac{24}{R^5} \sum_{M=-2}^{2} \frac{\hat{Q}_2^M(\hat{r}_A)\hat{Q}_2^{-M}(\hat{r}_B)}{(2+M)!(2-M)!}. \quad (8)$$

The Hamiltonian has the form of a sum of tensor products, composed of operators acting in subspaces of the unperturbed eigenstates of A and B. Usually, the 2^L-pole tensor components $\hat{q}_L^{M'}$ of a charge distribution are defined in its proper CS, that is, $X_A Y_A Z_A$ for the dimer A. Therefore, the $\hat{Q}_L^M$ tensor components in the T-CS are written as

$$\hat{Q}_L^M = \sum_{M'=-L}^{L} d_{MM'}^L(\delta)\hat{q}_L^{M'}, \quad (9)$$

where $d_{MM'}^L(\delta)$ are the reduced Wigner matrix elements. In the case of the alkali-metal dimer in the $^1\Sigma_g^+$ state, the only nonzero component of the quadrupole moment is $\hat{q}_2^0$ and Eq. (9) reduces to

$$\hat{Q}_2^M = d_{M0}^2(\delta)\hat{q}_2^0. \quad (10)$$

The component $\hat{q}_2^0$ is just a scalar parameter, which in what follows is referred to as q_2^0.

In the T-CS, the wave function of the rotational state of the dimer $|jm_j\rangle$ is written as $\sqrt{(2j+1)/2}d_{m_j0}^j(\delta)$, depending only on the internal angle δ. The normalization constant is such that the integral over angle δ is unity. We obtain the following expression for matrix elements of the operator $\hat{Q}_2^M$:

$$\langle jm_j'|\hat{Q}_2^M|jm_j\rangle = \frac{2j+1}{2}q_2^0 \int_0^\pi \sin\delta d\delta \, d_{m_j'0}^j(\delta) \, d_{M0}^2(\delta) \, d_{m_j0}^j(\delta)$$
$$= C_{20j0}^{j0} C_{2Mjm}^{jm_j'} q_2^0, \quad (11)$$

where the Clebsch-Gordan coefficients $C_{\ell m \ell' m'}^{\ell'' m''}$ appear after integrating the product of three $d_{MM'}^L$ functions [49]. The zeroth-order energy E_0^0 depends on j and is degenerate for all values of m_j. Thus, the perturbation Hamiltonian [Eq. (8)] has to be evaluated with the degenerate perturbation theory. Indeed, Eq. (11) shows that the quadrupole moment has matrix elements for different values of m_j because of the $m_j' = m_j + M$ selection rule. The degeneracy between different m_j values will be removed, leading to different values of C_5. This is the key point of the present treatment, as anisotropic values of C_5 are determined as functions of quantum numbers of the partners and not restricted to a given geometry.

Assuming the alkali-metal atom are in the state labeled $|n\ell\lambda\rangle$ (the spin is neglected here), we calculate the matrix elements of the atomic quadrupole moment operator for a given ℓ between two different Zeeman sublevels λ and λ' following the same treatment as previously. We obtain

$$\langle n\ell\lambda'|\hat{Q}_2^M|n\ell\lambda\rangle = -\sqrt{\frac{4\pi}{5}} \langle r_{n\ell}^2 \rangle \int_0^{2\pi} \sin\theta d\phi \int_0^\pi d\theta \, Y_\ell^{\lambda'*} Y_2^M Y_\ell^\lambda, \quad (12)$$

where the negative sign comes from the electron charge. The mean squared position $\langle r_{n\ell}^2 \rangle$ of the valence electron is independent of λ. Using the properties of spherical harmonics, we rewrite Eq. (12) as

$$\langle n\ell\lambda'|\hat{Q}_2^M|n\ell\lambda\rangle = -C_{20\ell0}^{\ell0} C_{2M\ell\lambda}^{\ell\lambda'} \langle r_{n\ell}^2 \rangle. \quad (13)$$

The situation is analogous to the molecular case: If $M \neq 0$, the operator $\hat{Q}_2^M$ couples λ to $\lambda' = \lambda + M$, and the perturbation Hamiltonian lifts the degeneracy with respect to λ also.

Summarizing the preceding results, the perturbation operator of Eq. (8) couples the $(2j+1)$ rotational states of the molecule with a given value of j and the $(2\ell+1)$ Zeeman states of the atom with a given value of ℓ. The C_5 coefficients are then given by $(2j+1) \times (2\ell+1)$ eigenvalues of the operator $\hat{V}_{AB}^{qq}$. Using Eqs. (11) and (13), the matrix elements of $\hat{V}_{AB}^{qq}$ are written

$$\langle jm_j'\ell\lambda'|V_{AB}^{qq}|jm_j\ell\lambda\rangle = -24C_{20j0}^{j0} C_{20\ell0}^{\ell0} \frac{q_2^0 \langle r_{n\ell}^2 \rangle}{R^5}$$
$$\times \sum_{M=-2}^{2} \frac{C_{2Mjm_j}^{jm_j'} C_{2-M\ell\lambda}^{\ell\lambda'}}{(2+M)!(2-M)!}. \quad (14)$$

From the integration over Euler angles and the properties of Clebsch-Gordan coefficients, the following selection rules for $\hat{V}_{AB}^{qq}$ are derived: (1) The projection $\widetilde{m}_J$ of the total orbital momentum $\vec{J} = \vec{j} + \vec{\ell}$ on the laboratory $\widetilde{z}$ axis is conserved. (2) The projection $m_J = m_j + \lambda$ of the total orbital momentum $\vec{J}$ on the Z axis of T-CS is conserved. This rule can also be deduced by the combination of Eqs. (11) and (13).

Equation (14) demonstrates the equivalence between the atomic orbital momentum $\vec{\ell}$ and the dimer rotation $\vec{j}$ in the formalism, which describes long-range interaction between two charge distributions with defined angular momenta irrespective to their internal structure. If one of the two angular momenta is zero, the corresponding quadrupole moment vanishes, and the C_5 coefficient as well. Therefore, the interaction will be the usual C_6/R^6 van der Waals potential. If neither of the two angular momenta j and ℓ is zero, the long-range interaction varies as C_5/R^5 and, therefore, the potential has a larger density of vibrational states close to the dissociation limit than the lowest electronic state of the system when the atom in its ground S state. Such a situation is favorable for the PA of atom-molecule pairs into excited trimers, just like for the PA of identical atom pairs (see, for example, experimental work of Ref. [50]).

IV. RESULTS AND DISCUSSION

To illustrate the previous formalism, we first consider analytically the simplest case $j = \ell = 1$. The perturbation Hamiltonian V_{AB}^{qq} reduces to a 9×9 matrix with elements calculated from tensor products of the atomic and dimer states. For simplicity, we omit the j and ℓ labels in the following, and the quantum states of the atom-molecule pair are denoted by projections $\{|m_j,\lambda\rangle\}$ only. All such states form the basis of the representation. If we sort the states by values of the conserved projection of the angular momentum $m_J = m_j + \lambda$, we obtain the matrix of V_{AB}^{qq} in a block-diagonal form.

The two blocks defined by $|m_j, \lambda\rangle = |-1, -1\rangle$ and $|+1, +1\rangle$ ($m_J = \pm 2$) reduce to a single element with a negative value of the corresponding coefficient

$$C_5 = -\frac{6 q_2^0 \langle r_{n\ell=1}^2 \rangle}{25}. \tag{15}$$

It produces an attractive interaction. Two other 2×2 blocks (with $m_J = \pm 1$) are defined by the two subspaces $\{|-1,0\rangle; |0,-1\rangle\}$ and $\{|0,1\rangle; |1,0\rangle\}$. The corresponding C_5 coefficients are $\frac{24 q_2^0 \langle r_{n\ell}^2\rangle}{25}$ (positive value) and zero. Finally, the last 3×3 block comes from the subspace $\{|-1,1\rangle; |0,0\rangle; |1,-1\rangle\}$ ($m_J = 0$). Two of the corresponding C_5 coefficients are zero, and the third one is

$$C_5 = -\frac{36 q_2^0 \langle r_{n\ell=1}^2 \rangle}{25}, \tag{16}$$

with the eigenvector $\frac{1}{\sqrt{6}}(|-1,1\rangle + 2|0,0\rangle + |1,-1\rangle)$. The coefficient in Eq. (16) is negative with the largest magnitude out of all C_5 coefficients obtained in the case of $j = \ell = 1$. It corresponds to the most attractive configuration between the atom and the dimer and is expected to be the most favorable for the PA.

The results of the calculation for the case $j = \ell = 1$ are summarized in Table I. The second column of the table gives the eigenvectors $|\Phi_0^0\rangle$ of the Hamiltonian of Eq. (8) in the $j = 1$ subspace. The third column gives the so-called *reduced* values of C_5 in units of $q_2^0 \langle r_{n\ell}^2\rangle$, which stresses the general character of our treatment: It can be applied to all alkali-metal trimers, but it can also be compared with the existing results on the long-range interaction between two excited atoms [39]. The eigenvectors obtained here are the same as in Ref. [39], but the signs of the C_5 coefficients are opposite to the coefficients obtained in Ref. [39]. The reason is clear from Eqs. (11) and (12): The signs of the matrix elements of quadrupole moments for the dimer Eq. (11) and the atom Eq. (12) are opposite. When they are combined together in Eq. (8) they give an additional negative sign to the perturbation. The two matrix

elements of the atomic quadrupoles give the positive sign to the perturbation matrix elements.

The fourth column in Table I displays estimates for the C_5 coefficients for $Cs_2 + Cs$. To the best of our knowledge, there are no available values for the quadrupole moment of Cs_2 in the literature. Therefore, we calculated it for the electronic ground state with the Gaussian quantum chemistry package [51] using the second-order Møller-Plesset method with the second definition of the triple-zeta-valence basis with polarization functions (so-called Def2-TZVPP), defined in Ref. [52]. To check the accuracy of such an estimation, we first calculated the quadrupole moment of K_2 and compared it to available accurate *ab initio* calculations [53]. We obtained 12.258 a.u., which differs by a factor 1.28 from the value 15.689 a.u. of Ref. [53]. For cesium, the Def2-TZVPP basis [52] contains also effective core potentials (ECPs) standing for the 46 inner electrons of the core. We obtained for Cs_2 the value of 14.51 a.u. that we multiplied by the same factor to estimate the Cs_2 quadrupole moment to $q_2^0 = 18.58$ a.u. The mean squared radius of the $6P$ orbital of cesium, which is 62.65 a.u., is calculated using a Dirac-Fock method [54]. It is worth mentioning that the values of C_5 shown in the table are of the same order of magnitude as the values for $Cs(6\,^2P) + Cs(6\,^2P)$ [39].

For $\ell = 1$ and arbitrary j, the perturbation Hamiltonian is a $3(2j+1) \times 3(2j+1)$ matrix, which can be diagonalized numerically. The eigenvalues obtained numerically for $j = 2$–4 are given in Table II. The C_5 coefficients are of the same order of magnitude as for $j = 1$, but on average they become smaller in magnitude as j increases, due to smaller Clebsch-Gordan

TABLE I. Values of the C_5 coefficient and their corresponding eigenvectors characterized by their m_J value, for $Cs_2(X\,^1\Sigma_g^+, v_d = 0, j = 1) + Cs(6\,^2P)$. The values of C_5 are given in units of $q_2^0 \langle r_{n\ell}^2\rangle$ in the third column, and in atomic units for $Cs_2 + Cs$ in the fourth column. For cesium, the data are $\langle r_{6p}^2\rangle = 62.65$ a.u. and $q_2^0 = 18.56$ a.u. (see text). Due to the uncertainty over q_2^0, the results are given with a precision of 1 a.u.

m_J	$|\Phi_0^0\rangle$	C_5 ($q_2^0 \langle r_{n\ell}^2\rangle$)	C_5 (a.u.)
-2	$|-1,-1\rangle$	$-\frac{6}{25}$	-279
-1	$\frac{1}{\sqrt{2}}(|-1,0\rangle + |0,-1\rangle)$	$\frac{24}{25}$	1116
-1	$\frac{1}{\sqrt{2}}(|-1,0\rangle - |0,-1\rangle)$	0	0
0	$\frac{1}{\sqrt{6}}(|-1,1\rangle + 2|0,0\rangle + |1,-1\rangle)$	$-\frac{36}{25}$	-1674
0	$\frac{1}{\sqrt{3}}(|-1,1\rangle - |0,0\rangle + |1,-1\rangle)$	0	0
0	$\frac{1}{\sqrt{2}}(|-1,1\rangle - |1,-1\rangle)$	0	0
$+1$	$\frac{1}{\sqrt{2}}(|1,0\rangle - |0,1\rangle)$	$\frac{24}{25}$	1116
$+1$	$\frac{1}{\sqrt{2}}(|1,0\rangle + |0,1\rangle)$	0	0
$+2$	$|1,1\rangle$	$-\frac{6}{25}$	-279

TABLE II. The C_5 coefficients of the $Cs_2(X\,^1\Sigma_g^+, v_d = 0, j) + Cs(6\,^2P)$ long-range interaction calculated numerically for $j = 2$–4. C_5 are sorted by projections $m_J = m_j + \lambda$ of the total orbital angular momentum on the Z axis, and by the sign $+ (-)$ of the wave function with respect to a reflection through the plane containing the Z axis. In analogy to a diatomic molecule, the eigenstates are labeled with $\Sigma^{+/-}, \Pi, \Delta, \Phi, \Gamma$, and H for $m_J = 0,1,2,3,4,5$, respectively. The values for $\langle r_{6p}^2\rangle$ and q_2^0 are the same as in Table I.

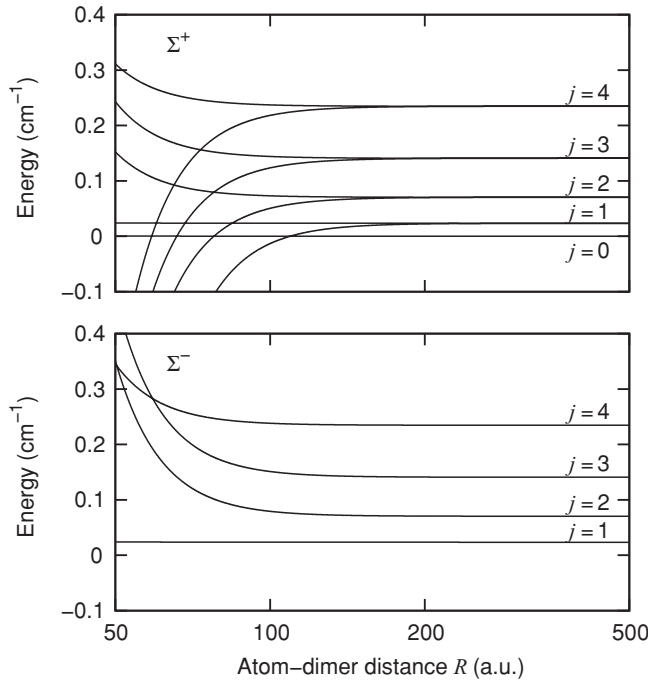| Symmetry	j	C_5 (a.u.)	Symmetry	j	C_5 (a.u.)
Σ^+	2	-913	Δ	2	-140
	2	116		2	1136
	3	-796		3	-835
	3	145		3	-87
	4	-755		3	736
	4	157		4	-721
Σ^-	2	399		4	-11
	3	465		4	623
	4	489	Φ	2	-399
Π	2	-964		3	-245
	2	-19		3	1175
	2	584		4	-783
	3	-783		4	-161
	3	64		4	835
	3	532	Γ	3	-465
	4	-739		4	-320
	4	108		4	1208
	4	522	H	4	-507

FIG. 2. Long-range potential energy curves C_5/R^5 as a function of the atom-dimer distance R (notice logarithmic scale along R), for the Σ^+ and Σ^- symmetries, and for the five lowest rotational levels of $Cs_2[X\,^1\Sigma_g^+(v_d = 0)]$. The curves are drawn for distances larger than the Le Roy radius $R_{LR} = 45$ a.u.

coefficients. The C_5 coefficients are sorted by values of $|m_J|$, which, in analogy to diatomic molecules, are labeled Σ, Π, Δ, Φ, Γ, and H for $|m_J| = 0$ to 5, respectively. For Σ states, the reflection symmetry through the Z axis is also considered, giving the usual $+$ $(-)$ superscripts. For states other than Σ the sign $+$ $(-)$ is not specified because such states are degenerate (in the present approximation) with respect to the reflection.

We use the same symmetry notations in Figs. 2, 3, and 4, where we display the long-range potential energy curves C_5/R^5 for the $Cs_2 + Cs(6\,^2P)$ system calculated for the first five rotational levels j of Cs_2 as a function of the atom-dimer distance R. The energies of dissociation are given by Cs_2 rotational energies, $B_0 j (j + 1)$, $j = 0, \ldots, 4$. The rotational constant for ground vibrational level of Cs_2 is $B_0 = 1.173\,14 \times 10^{-2}$ cm^{-1} [55].

The potential energy curves are shown up to $R = 500$ a.u. Beyond this limit, the distance between Cs_2 and Cs becomes comparable to the wavelengths of relevant atomic and molecular transitions, which are in the optical frequency domain. Therefore, in that region, electrodynamics effects, for example, due to retardation, should be taken into account [56].

As already mentioned, the lower limit of the region where the present approximation is applicable can be estimated by the Le Roy radius $R_{LR} = 2(\sqrt{\langle r_0^2(Cs_2)\rangle} + \sqrt{\langle r_{6p}^2(Cs)\rangle})$, where $\langle r_0^2\rangle$ and $\langle r_{6p}^2\rangle$ are related to the extension of the dimer and atomic electronic clouds, respectively. For the atom, one has $\langle r_{6P}^2\rangle = 62.65$ a.u., which is given in Table I. As for the dimer, $\langle r_0^2\rangle$ is calculated from the elements of the quadrupole tensor. All its nondiagonal elements $Q_{\alpha\beta}$ are zero for $^1\Sigma_g^+$
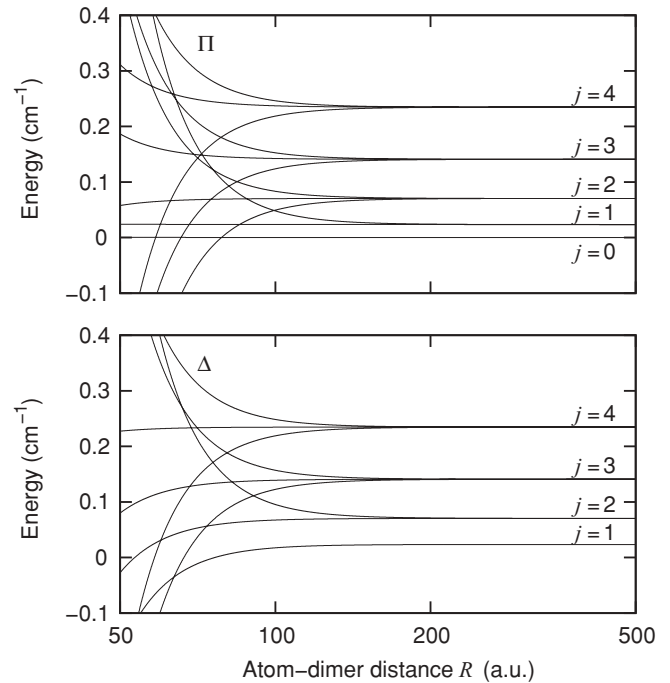

FIG. 3. Same as Fig. 2 for Π and Δ symmetries.

states in D-CS. Its diagonal elements $Q_{\alpha\alpha}$ ($\alpha = X_A, Y_A$, or Z_A) in D-CS are estimated using the GAUSSIAN package and can be formally written as a sum over all charges:

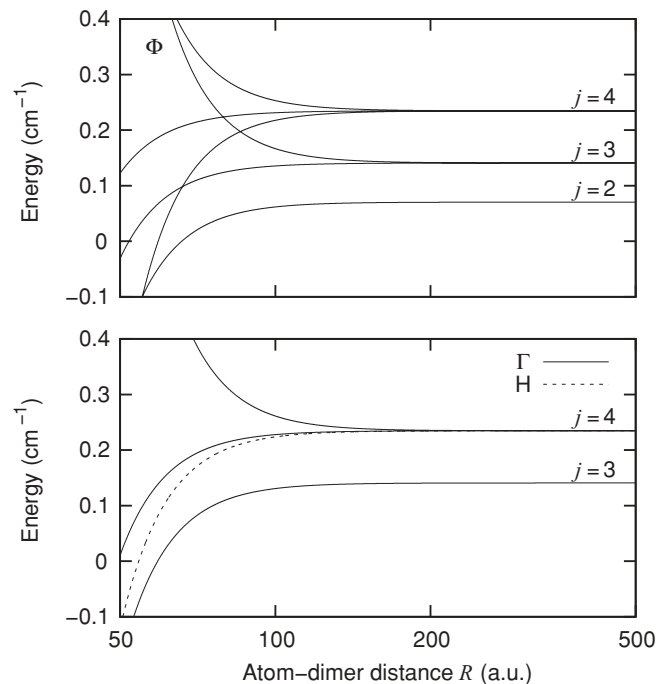$$Q_{\alpha\alpha} = \sum_i q_i \langle\alpha_i^2\rangle. \qquad (17)$$

FIG. 4. Same as Fig. 2 for Φ, Γ, and H symmetries. The top panel displays Φ symmetry, and the bottom one displays both Γ symmetry (solid lines) and H symmetry (dashed lines).

As the two nuclei of Cs_2 are along the Z_A axis and it is a $^1\Sigma_g^+$ molecular state, $Q_{X_A X_A}$ is equal to $Q_{Y_A Y_A}$ and both are functions of the coordinates of two valence electrons only ($i = 1,2$):

$$Q_{X_A X_A} = -e \sum_{i=1}^{2} \langle X_{Ai}^2 \rangle. \tag{18}$$

Now considering for simplicity that the cores are fixed at the position $Z_A = \pm r_e/2$ (the rigid rotor approximation, valid for $v_d = 0$), for $Q_{Z_A Z_A}$ we obtain

$$Q_{Z_A Z_A} = e \frac{r_e^2}{2} - e \sum_{i=1}^{2} \langle Z_{Ai}^2 \rangle. \tag{19}$$

Now, setting

$$\langle r_0^2 \rangle = \sum_{i=1}^{2} \sum_{\alpha=(X_A,Y_A,Z_A)} \langle \alpha_i^2 \rangle, \tag{20}$$

we reach the final expression for $\langle r_0^2 \rangle$,

$$\langle r_0^2 \rangle = \frac{r_e^2}{2} - Q_{Z_A Z_A} - 2Q_{X_A X_A}, \tag{21}$$

where $e = 1$ in atomic units. The $Q_{\alpha\alpha}$ matrix elements are calculated with the same method as q_2^0 (using the ratio 1.27 to the K_2 value),[1] which yields $Q_{X_A X_A} = -69$ a.u., $Q_{Z_A Z_A} = -41$ a.u., and $r_e = 8.7$ a.u. Therefore, we obtain $\langle r_0^2 \rangle = 216$ a.u. and the Le Roy radius $R_{LR} = 45$ a.u.

As we can see from Figs. 2, 3, and 4, the Le Roy radius is smaller than the distance at which the curves start to cross each other. This is the second main result of the article. Unlike the case of two atoms, the rotational structure of the dimer is small enough to compete with the quadrupole-quadrupole interaction. The lower limit of R_m for the applicability of the present perturbation approach is thus fixed by the crossing of the potential energy curves. In order to estimate R_m, we note that the first crossing occurs between the curves dissociating toward to the $j = 0$ limit and from the most attractive curve corresponding to $j = 1$. Putting $2B_0 \equiv C_5^m/R_m^5$ yields a general estimate for R_m [see Eq. (16)]:

$$R_m \sim \left(\frac{C_5^m}{2B_0} \right)^{1/5} = \left(\frac{18 q_2^0 \langle r_{n\ell}^2 \rangle}{25 B_0} \right)^{1/5}$$

$$\approx 0.936 \times \left(\frac{q_2^0 \langle r_{n\ell}^2 \rangle}{B_0} \right)^{1/5}. \tag{22}$$

For cesium, Eq. (22) yields $R \approx 102$ a.u. In the rigid rotor approximation with $B_0 = 1/(2\mu r_e^2)$ and where μ is the reduced mass of the dimer, Eq. (22) shows that the value of R_m is smaller for lighter atoms. For example, replacing in our treatment Cs by ^6Li with the atomic parameters $\langle r_{2p}^2 \rangle = 32.5$ a.u. [57], $r_e = 5.05$ a.u., and $q_2^0 = 10.7$ a.u [53], we obtain $R_m = 43$ a.u. This value of R_m is larger than the Le

Roy radius for lithium, for which we obtained 26 a.u. using Eq. (21).

For distances such that $R_{LR} < R < R_m$, the long-range potential (1) is still valid, but not the perturbative approach. The nonadiabatic interaction at the curve crossings (for a given symmetry) is expected to be strong. In particular, the interaction between permanent quadrupoles would couple the dimer rotational level j with $j' = j \pm 2$, $j \pm 4$ near the crossings. Higher-order contributions in $1/R$ should also be considered.

The number N of partial waves involved in the atom-dimer collisions depends on the temperature in the actual experiment. In order to give an upper bound for N, we consider a potential curve with the most attractive C_5, given by Eq. (16) and with the added centrifugal term. It is straightforward to show that the height of the potential barrier E_N^{max} for a given N is

$$E_N^{max} = \frac{9}{20} \left(\frac{5}{24} \right)^{2/3} \left(\frac{N(N+1)}{m} \right)^{5/3} \left(q_2^0 \langle r_{n\ell}^2 \rangle \right)^{-2/3}$$

$$\approx 0.158 \times \left(\frac{N(N+1)}{m} \right)^{5/3} \left(q_2^0 \langle r_{n\ell}^2 \rangle \right)^{-2/3}, \tag{23}$$

where m is the mass of a single atom. Converted to the temperature, E_N^{max} is approximately 1 μK for cesium. If we take typical temperatures 10–100 μK for which PA experiments are achieved, only a few partial waves (6 $\sim$ 7 for the present case) will play a significant role in collisions. This contrasts with the PA of identical atom pairs, interacting with a long-range R^{-3} potential which allow much more partial waves than here.

V. CONCLUSIONS AND PERSPECTIVES

In this article, we used the multipolar expansion to calculate the long-range interaction energy of a diatomic molecule in its electronic ground state and in an arbitrary rovibrational level and an excited atom. We applied our treatment to the case of a ground-state Cs_2 molecule and an excited $Cs(6\,^2P)$ atom, as a prospect for cold-atom–molecule PA. The dimer and the atom interact through their permanent quadrupole moment. In contrast with previous works, the anisotropic interaction is computed for arbitrary geometries of the atom-molecule pair and depends on their internal quantum numbers. We showed that the interaction lifts the degeneracy over their respective magnetic sublevels. Using the degenerate perturbation theory, we calculated the C_5 coefficients characterizing the quadrupole-quadrupole interaction for the five lowest rotational levels of the ground-state dimer. The PA of a ground-state $X\,^1\Sigma_g^+$ alkali-metal dimer molecule with a ground state $n\,^2S$ alkali-metal atom is found possible by exciting the dimer-atom system with a laser frequency red detuned from the $n\,^2S \to n\,^2P$ atomic transitions.

We demonstrated that the small-R limit of applicability of our treatment is not due to the overlap of the electronic clouds of the partners, as in the atom-atom case, but to the competition between the rotational energy of the dimer and the long-range quadrupole-quadrupole interaction. This induces crossings between potential energy curves corresponding to different rotational levels. In the region $50 \leqslant R \leqslant 100$ a.u.,

---

[1]The q_2^0 and $Q_{\alpha\alpha}$ elements are connected to each other by $q_2^0 = 2Q_{Z_A Z_A} - Q_{X_A X_A} - Q_{Y_A Y_A}$.

the multipolar expansion is still valid but not the perturbation approach. The inclusion of nonadiabatic couplings is required in this region for an appropriate description of the long-range behavior, as well as higher-order effects in $1/R$. This will be discussed in detail in a forthcoming presentation.

It is important to stress that the preceding treatment has been developed in the framework of the LS coupling case in order to keep our description simple. The next step is to account for the fine structure of the excited atom. The main difference with the formulas reported here will be the change of the atomic state from $P \equiv |n, \ell, \lambda\rangle$ to $P_j \equiv |n, \ell, j, \lambda_j\rangle$ (with $j = 1/2$ or $3/2$), where the state P_j is written as the appropriate superposition of atomic states with different λ and spin projections through a unitary transformation. We note, however, that for most of the alkali-metal atoms (from Na to Cs) the fine structure is much larger than the magnitude of the long-range atom-dimer interaction. Therefore, the related C_5 coefficients will result from linear combinations of the coefficients of Table II and will not modify the main statement of our study concerning the range of validity of our approach. In contrast, the case of a lithium atom will be remarkable as its small fine structure of 0.335 cm^{-1} [58] falls within the range of energies displayed in Figs. 2–4, and is expected to modify the present conclusions. This work is currently in progress. A similar discussion obviously holds for the hyperfine interaction of the excited atom, which will induce even more complexity in the formalism. It could safely be neglected for all species except for cesium (the hyperfine splitting of the $6\,^2P_{1/2}$ level is $1.167\,688(81)$ GHz [59]).

The present formalism can be generalized to PA of dipolar dimers and atoms, like KRb with K or KRb with Rb. If the atom is in the excited state $n\,^2P$ and the heteronuclear dimer in an excited rotational state $j > 0$, the long-range dimer-atom interaction is dominated by a dipole-quadrupole term varying as C_4/R^4. The long-range interaction between two identical dipolar molecules can also be treated in the same way, as the leading term will be the usual van der Waals C_6/R^6 term if both molecules are in their lowest rotational level $j = 0$ or dipole-dipole C_3/R^3 term if one of them is rotationally excited. One could thus investigate the PA of two identical heteronuclear KRb ground-state molecules in their lowest vibrational level using a laser field with a frequency red detuned with respect to $j = 0 \rightarrow j = 1$ transition. In this respect, PA of two dimers is very similar to the PA of two identical alkali-metal atoms, except that the laser frequency is much smaller for the two-dimer PA.

[1] H. R. Thorsheim, J. Weiner, and P. S. Julienne, Phys. Rev. Lett. **58**, 2420 (1987).

[2] P. D. Lett, K. Helmerson, W. D. Phillips, L. P. Ratliff, S. L. Rolston, and M. E. Wagshul, Phys. Rev. Lett. **71**, 2200 (1993).

[3] J. D. Miller, R. A. Cline, and D. J. Heinzen, Phys. Rev. Lett. **71**, 2204 (1993).

[4] P. D. Lett, P. S. Julienne, and W. D. Philips, Annu. Rev. Phys. Chem. **46**, 423 (1995).

[5] W. Stwalley and H. Wang, J. Mol. Spectrosc. **195**, 194 (1999).

[6] K. M. Jones, E. Tiesinga, P. D. Lett, and P. S. Julienne, Rev. Mod. Phys. **78**, 483 (2006).

[7] O. Dulieu and C. Gabbanini, Rep. Prog. Phys. **72**, 086401 (2009).

[8] K. M. Jones, P. S. Julienne, P. D. Lett, W. D. Phillips, E. Tiesinga, and C. J. Williams, Europhys. Lett. **35**, 85 (1996).

[9] H. Wang, P. L. Gould, and W. Stwalley, J. Chem. Phys. **106**, 7899 (1997).

[10] A. Fioretti, D. Comparat, C. Drag, C. Amiot, O. Dulieu, F. Masnou-Seeuws, and P. Pillet, Eur. Phys. J. D **5**, 389 (1999).

[11] D. Comparat, C. Drag, B. L. Tolra, A. Fioretti, P. Pillet, A. Crubellier, O. Dulieu, and F. Masnou-Seeuws, Eur. Phys. J. D **11**, 59 (2000).

[12] A. Fioretti, C. Amiot, C. M. Dion, O. Dulieu, M. Mazzoni, G. Smirne, and C. Gabbanini, Eur. Phys. J. D **15**, 189 (2001).

[13] M. Movre and G. Pichler, J. Phys. B **10**, 2631 (1977).

[14] W. C. Stwalley, Y. H. Uang, and G. Pichler, Phys. Rev. Lett. **41**, 1164 (1978).

[15] N. Bouloufa, A. Crubellier, and O. Dulieu, Phys. Scr., T **134**, 014014 (2009).

[16] A. Fioretti, D. Comparat, A. Crubellier, O. Dulieu, F. Masnou-Seeuws, and P. Pillet, Phys. Rev. Lett. **80**, 4402 (1998).

[17] A. N. Nikolov, E. E. Eyler, X. T. Wang, J. Li, H. Wang, W. C. Stwalley, and P. L. Gould, Phys. Rev. Lett. **82**, 703 (1999).

[18] C. Gabbanini, A. Fioretti, A. Lucchesini, S. Gozzini, and M. Mazzoni, Phys. Rev. Lett. **84**, 2814 (2000).

[19] F. K. Fatemi, K. M. Jones, P. D. Lett, and E. Tiesinga, Phys. Rev. A **66**, 053401 (2002).

[20] D. Wang, J. Qi, M. F. Stone, O. Nikolayeva, H. Wang, B. Hattaway, S. D. Gensemer, P. L. Gould, E. E. Eyler, and W. C. Stwalley, Phys. Rev. Lett. **93**, 243005 (2004).

[21] C. Haimberger, J. Kleinert, M. Bhattacharya, and N. P. Bigelow, Phys. Rev. A **70**, 021402 (2004).

[22] A. J. Kerman, J. M. Sage, S. Sainis, T. Bergeman, and D. DeMille, Phys. Rev. Lett. **92**, 153001 (2004).

[23] M. W. Mancini, G. D. Telles, A. R. L. Caires, V. S. Bagnato, and L. G. Marcassa, Phys. Rev. Lett. **92**, 133203 (2004).

[24] S. D. Kraft, P. Staanum, J. Lange, L. Vogel, R. Wester, and M. Weidemüller, J. Phys. B **39**, S993 (2006).

[25] M. T. Cvitaš, P. Soldán, J. M. Hutson, P. Honvault, and J.-M. Launay, Phys. Rev. Lett. **94**, 200402 (2005).

[26] N. Zahzam, T. Vogt, M. Mudrich, D. Comparat, and P. Pillet, Phys. Rev. Lett. **96**, 023202 (2006).

[27] P. Staanum, S. D. Kraft, J. Lange, R. Wester, and M. Weidemüller, Phys. Rev. Lett. **96**, 023201 (2006).

[28] E. R. Hudson, N. B. Gilfoy, S. Kotochigova, J. M. Sage, and D. DeMille, Phys. Rev. Lett. **100**, 203201 (2008).

[29] S. Knoop, F. Ferlaino, M. Berninger, M. Mark, H.-C. Nägerl, R. Grimm, J. P. D'Incao, and B. D. Esry, Phys. Rev. Lett. **104**, 053201 (2010).

[30] S. Ospelkaus, K.-K. Ni, D. Wang, M. H. G. de Miranda, B. Neyenhuis, G. Quéméner, P. S. Julienne, J. Bohn, D. S. Jin, and J. Ye, Science **327**, 853 (2010).

[31] S. Ospelkaus, D. Wang, G. Quéméner, B. Neyenhuis, M. H. G. de Miranda, J. L. Bohn, J. Ye, D. S. Jin, and K.-K. Ni, Nature (London) **464**, 1324 (2010).

[32] N. P. Mehta, S. T. Rittenhouse, J. P. D'Incao, J. von Stecher, and C. H. Greene, Phys. Rev. Lett. **103**, 153201 (2009).

[33] J. Levinsen, T. G. Tiecke, J. T. M. Walraven, and D. S. Petrov, Phys. Rev. Lett. **103**, 153202 (2009).

[34] V. Efimov, Phys. Lett. B **33**, 563 (1970).

[35] V. Efimov, Nature Phys. **5**, 533 (2010).

[36] T. Kraemer, M. Mark, P. Waldburger, J. G. Danzl, C. Chin, B. Engeser, A. D. Lange, K. Pilch, A. Jaakkola, H.-C. Nägerl, and R. Grimm, Nature (London) **440**, 315 (2006).

[37] S. E. Pollack, D. Dries, and R. G. Hulet, Science **326**, 1683 (2009).

[38] M. Zaccanti, B. Deissler, C. D'Errico, M. Fattori, M. Jona-Lasinio, S. Müller, G. Roati, M. Inguscio, and G. Modugno, Nat. Phys. **5**, 586 (2009).

[39] M. Marinescu, Phys. Rev. A **56**, 4764 (1997).

[40] C. Pouchan and M. Rérat, Chem. Phys. Lett. **257**, 409 (1996).

[41] M. Rérat and B. Bussery-Honvault, Mol. Phys. **101**, 373 (2003).

[42] M. Mérawa, M. Rérat, and B. Bussery-Honvault, J. Mol. Struct. (Theochem) **633**, 137 (2003).

[43] B. Bussery-Honvault, F. Dayou, and A. Zanchet, J. Chem. Phys. **129**, 234302 (2008).

[44] B. Bussery-Honvault and F. Dayou, J. Phys. Chem. A **113**, 14961 (2009).

[45] D. V. M. R. Flannery and V. N. Ostrovsky, J. Phys. B **38**, S279 (2005).

[46] G. C. Groenenboom, X. Chu, and R. V. Krems, J. Chem. Phys. **126**, 204306 (2007).

[47] R. J. LeRoy, Can. J. Phys. **52**, 246 (1974).

[48] B. Ji, C.-C. Tsai, and W. C. Stwalley, Chem. Phys. Lett. **236**, 103 (1995).

[49] D. A. Varshalovich, A. N. Moskalev, and V. K. Khersonskii, *Quantum Theory of Angular Momentum* (World Scientific, Singapore, 1988).

[50] P. Pillet, A. Crubellier, A. Bleton, O. Dulieu, P. Nosbaum, I. Mourachko, and F. Masnou-Seeuws, J. Phys. B **30**, 2801 (1997).

[51] M. J. Frisch *et al.*, *Gaussian 03, Revision D.02* (Gaussian, Wallingford, CT, 2004).

[52] F. Weigend and R. Ahlrichs, Phys. Chem. Chem. Phys. **7**, 3297 (2005).

[53] J. F. Harrison and D. B. Lawson, Int. J. Quantum Chem. **102**, 1087 (2005).

[54] M. Aymar (private communication).

[55] C. Amiot and O. Dulieu, J. Chem. Phys. **117**, 5155 (2002).

[56] H. B. G. Casimir and D. Polder, Phys. Rev. **73**, 360 (1948).

[57] J. Pipin and D. M. Bishop, Phys. Rev. A **45**, 2736 (1992).

[58] L. J. Radziemski, R. Engleman, and J. W. Brault, Phys. Rev. A **52**, 4462 (1995).

[59] T. Udem, J. Reichert, R. Holzwarth, and T. W. Hänsch, Phys. Rev. Lett. **82**, 3568 (1999).